JOURNAL OF Materials CHEMISTRY

Charge disproportionation in iron(IV) oxides: electronic properties and magnetism in $Sr_3Fe_{2-x}Ti_xO_{7-y}$ annealed at high oxygen pressures

Peter Adler*

Max-Planck-Institut für Festkörperforschung, Heisenbergstr. 1, 70569 Stuttgart, Germany. E-mail: adler@vaxff2.mpi-stuttgart.mpg.de

Received 1st September 1998, Accepted 13th November 1998

It has been studied how partial substitution of formally $3d^4$ Fe^{IV} ions by $3d^0$ Ti^{IV} ions influences the charge-disproportionation state and magnetism in $Sr_3Fe_2O_7$. For this purpose Ruddlesden–Popper-type phases $Sr_3Fe_{2-x}Ti_xO_{7-y}$ have been synthesized from the oxides and, in order to reach high oxygen contents, annealed at oxygen pressures up to 70 MPa. The materials were investigated by X-ray powder diffractometry, ^{57}Fe Mössbauer spectroscopy, magnetic susceptibility, and electrical resistance measurements. From the *a*-lattice parameters it is derived that in spite of annealing the samples at high oxygen pressures a certain oxygen deficiency occurs which gives rise to an Fe^{III} fraction increasing with x. Mössbauer spectra evidence a charge disproportionation of Fe^{IV} in materials with $x=0.2$ and 0.5, whereas for $x=1.0$ and 1.5 a mixed-valence state is formed with an Fe^{III}/Fe^{IV} ratio as derived from sample composition. The isomer shifts and magnetic hyperfine fields suggest a collective electronic state with partial transfer of charge and spin density between the Fe sites in the charge-disproportionation phases. In the samples with $x=0.2$ and 0.5 the degree of charge and spin separation is increased in comparison with $Sr_3Fe_2O_7$. The electrical conductivity decreases with increasing x. The magnetism of all the materials is governed by ferro- and antiferro-magnetic exchange interactions which lead for decreasing temperature to a broad transition to an antiferromagnetic state for $x=0.2$ and to spin-glass behavior for materials with larger x.

1 Introduction

In recent years there has been a strong interest in the interplay between crystal structure, electronic states, magnetism, and electrical conductivity in transition metal oxides.[1] Particularly stimulating was the discovery of high-temperature superconductivity in mixed-valence oxocuprates and colossal magnetoresistance (CMR) effects in mixed-valence oxomanganates. An interesting class of compounds with respect to this interplay are iron(IV) oxides with perovskite-related structures which even in the absence of mixed valency can be considered as transition metal oxides at the insulator–metal borderline.[2,3] This view is suggested by the absence of a Jahn–Teller effect expected for a localized $3d^4$ high-spin configuration in compounds like $SrFeO_3$, $Sr_3Fe_2O_7$, and Sr_2FeO_4, by the high electronic conductivity of $SrFeO_3$,[4] the complicated magnetism of these materials involving ferromagnetic as well as antiferromagnetic exchange interactions,[5–7] and by pressure-induced electronic structure changes in the antiferromagnetic semiconductor Sr_2FeO_4 which result in an insulator–metal transition.[8,9] A further peculiarity in the electronic behavior of iron(IV) oxides is the occurrence of a charge-disproportionation state in $CaFeO_3$[10] and $Sr_3Fe_2O_7$[6] which was discovered by Mössbauer spectroscopy and, assuming integral oxidation states, has been formulated as $2\ Fe^{IV} \rightarrow Fe^{III} + Fe^{V}$. However, the continuous change from the $CaFeO_3$- to the $SrFeO_3$-type Mössbauer spectra in the solid solution series $Sr_{1-x}Ca_xFeO_3$ and the Mössbauer spectra of the system $Sr_{1-x}La_xFeO_3$[11] suggest rather a gradual charge disproportionation with non-integral oxidation states for the different iron sites.

In order to study the nature of this unusual electronic state in more detail we have recently reinvestigated the properties of $Sr_3Fe_2O_7$ and synthesized and characterized the substituted phases $Sr_{2.7}Ba_{0.3}Fe_2O_7$ **I** and $Sr_{2.6}La_{0.4}Fe_2O_7$ **II**.[3] The crystal structures of $Sr_3Fe_2O_7$[12] and the substituted materials are isotypic to the Ruddlesden–Popper phase $Sr_3Ti_2O_7$ and reveal a quasi two-dimensional network of perovskite double layers which are composed of corner-sharing FeO_6 octahedra. The charge disproportionation of Fe^{IV} was found to persist in **I** where the iron oxidation state remains unchanged as well as in **II** which is formally a mixed-valence compound with 80% Fe^{IV} and 20% Fe^{III}. The magnetism in all the materials involves ferro- and anti-ferromagnetic exchange interactions which in the case of **II** leads to spin-glass behavior below 50 K. The electronic conductivity in both substituted materials is smaller than in $Sr_3Fe_2O_7$. The detailed inspection of the Mössbauer isomer shifts and magnetic hyperfine fields supports an interpretation of the charge disproportionation in Fe^{IV} oxides as a collective electronic state with non-integral oxidation states of iron. In our previous substitution studies on $Sr_3Fe_2O_7$ the iron–oxygen network remained intact.

In the present contribution we report the synthesis of the materials $Sr_3Fe_{2-x}Ti_xO_{7-y}$ and their characterization by powder X-ray diffractometry, Mössbauer spectroscopy, magnetic susceptibility, and electrical resistance measurements. The aim of this work was to investigate how the electronic properties and the magnetism of the parent compound change when the Fe–O network is successively diluted by non-magnetic $3d^0$ Ti^{IV} ions. For this purpose it is desirable to retain all the Fe ions in the materials in the +4 oxidation state. However, although all samples were annealed under high oxygen pressures, a certain oxygen deficiency in the substituted materials could not be avoided. As a consequence an Fe^{III} content occurs which increases with increasing Ti content.

2 Experimental

Samples of $Sr_3Fe_{2-x}Ti_xO_{7-y}$ with $x=0.2$, 0.5, 1.0, and 1.5 were prepared from stoichiometric mixtures of the oxides SrO, Fe_2O_3, and TiO_2, which were ground in a ball mill, heated at 1100 °C in air overnight, reground, pelletized subsequently, and heated for a further 3 days at 1100 °C. For the materials with $x=1.0$ and 1.5 further regrinding and heating at 1200 °C was required. Finally, all materials were annealed at oxygen pressures of 60 MPa at 500 °C for 16 h and subsequently at 70 MPa and 350 °C for a further 16 h in an autoclave in order to minimize oxygen deficiency. The materials were

characterized by X-ray powder diffractometry (STOE powder diffractometer, monochromatic Cu-Kα_1 radiation) before and after high-pressure oxygen annealing. All samples were single phase with the exception of that with $x=1.0$ where a small amount of K_2NiF_4-type phase is seen in the X-ray powder diagram. In order to derive accurate lattice parameters, silicon was added as an internal standard.

Mössbauer spectra were measured with a conventional Mössbauer spectrometer. A ^{57}Co/Rh source (kept at room temperature) was moved with a sine-type drive signal, some spectra were recorded with a triangular drive signal. For low-temperature measurements the sample was placed in a cryostat which permits Mössbauer experiments down to 2 K. All isomer shifts tabulated in this work are referred to α-Fe.

Magnetic susceptibility measurements were performed with a SQUID susceptometer in an external magnetic field of 0.1 T. Zero-field cooled (ZFC) data were collected by heating the materials after cooling without magnetic field to about 5 K. Field-cooled (FC) data were obtained by cooling materials in the magnetic field. Diamagnetic contributions to the magnetic susceptibilities χ are negligible. Magnetic susceptibilities are given in emu mol^{-1}. Multiplying with $4\pi\times10^{-6}$ leads to the χ-values in SI units (m^3 mol^{-1}).

Electrical resistance measurements were performed on high-pressure oxygen annealed pellets of $Sr_3Fe_{2-x}Ti_xO_{7-y}$ using the four-point contact method. The resistances R were converted into specific conductivities σ.

3 Results

X-Ray powder diffractometry

The parent compounds $Sr_3Fe_2O_7$ and $Sr_3Ti_2O_7$ crystallize in the tetragonal space group $I4/mmm$. The X-ray powder diagrams of the mixed system $Sr_3Fe_{2-x}Ti_xO_{7-y}$ can also be indexed in this space group. Fig. 1 shows the lattice parameters a and c of the materials before and after annealing at high oxygen pressure. The data for stoichiometric $Sr_3Fe_2O_6$, $Sr_3Fe_2O_7$ and $Sr_3Ti_2O_7$ were taken from the literature.[12,13] Both lattice constants increase in a non-linear way with increasing Ti content x. Furthermore, for a given x one observes a decrease of a and c after high-pressure oxygen treatment. The increase in a and c with x is attributed to the replacement of smaller Fe^{IV} by larger Ti^{IV} ions. The decrease of a and c after high-pressure oxygen annealing evidences uptake of additional oxygen by the materials and is a consequence of a concomitant oxidation of larger Fe^{III} to smaller Fe^{IV} ions. It is noted that the decrease in a after high-pressure treatment normalized to the Fe concentration becomes smaller with increasing x.

The lattice parameters a, which correspond to the mean metal–metal distance in the ab plane of the crystal structure, may be used for estimating the Fe^{III} fractions and oxygen deficiencies for the materials if it is assumed that a depends linearly on the composition (Vegard's law). As every oxygen vacancy is accompanied by a reduction of two Fe^{IV} to Fe^{III} ions the composition of the Ti-substituted materials is given by $Sr_3Fe_{2-x-2y}{}^{IV}Fe_{2y}{}^{III}Ti_x{}^{IV}O_{7-y}$. Denoting the fraction of Fe^{III} sites as γ the a-lattice parameters of the samples are obtained by weighting the a parameters of $Sr_3Fe_2O_7$ [$a(Fe^{IV})$], $Sr_3Fe_2O_6$ [$a(Fe^{III})$] and $Sr_3Ti_2O_7$ [$a(Ti^{IV})$] according to

$$a=\frac{x}{2}a(Ti^{IV})+\left(1-\frac{x}{2}\right)[\gamma a(Fe^{III})+(1-\gamma)a(Fe^{IV})] \quad (1)$$

where γ is related to y by $\gamma=2y/(2-x)$. The Fe^{III} contents and oxygen compositions for the present materials estimated by this procedure are given in Table 1. They will be used later for correlation with the Mössbauer spectra. The Fe^{III} fractions of the air-annealed materials are between 45 and 60%. The degree of oxidation of Fe^{III} to Fe^{IV} achieved by high-pressure oxygen annealing decreases with increasing Ti^{IV} content. There is only a small Fe^{III} fraction of about 6% for the material with $x=0.2$, but the Fe^{III} fraction increases to about 33% for the material with $x=1$.

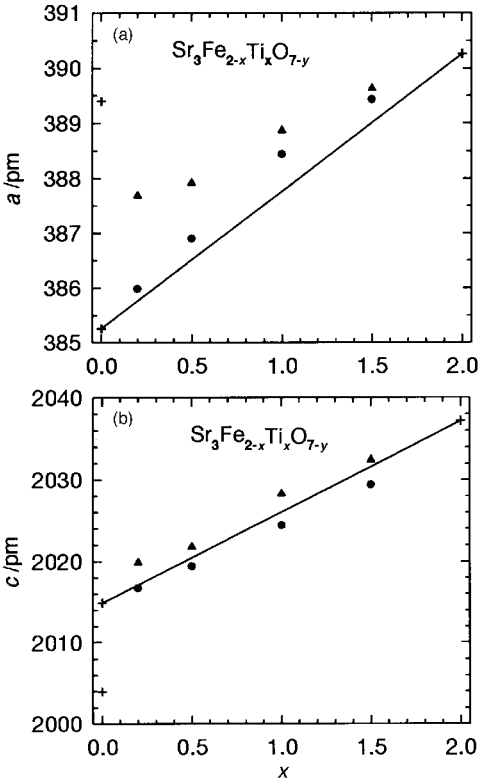

Fig. 1 Variation of the lattice parameters a (a) and c (b) with Ti content x for $Sr_3Fe_{2-x}Ti_xO_{7-y}$ before (▲) and after (●) high-pressure oxygen annealing. The values for $Sr_3Fe_2O_6$, $Sr_3Fe_2O_7$ and $Sr_3Ti_2O_7$ (+) were taken from ref. 12 and 13, respectively. The solid lines correspond to a linear interpolation between the a and c values of $Sr_3Fe_2O_7$ and $Sr_3Ti_2O_7$.

Table 1 Lattice parameters a, Fe^{III} fractions γ, and oxygen contents $7-y$ for $Sr_3Fe_{2-x}Ti_xO_{7-y}$ derived from X-ray powder data according to eqn. (1) with $a(Ti^{IV})=390.26$ pm,[13] $a(Fe^{IV})=385.25$ pa[12] and $a(Fe^{III})=389.40$ pm.[12] The error in γ is estimated to be $\leqslant0.05$, hp refers to high-pressure oxygen annealed samples

x	a/pm	γ	$7-y$
0.2	387.69(2)	0.52	6.53
0.2 hp	385.98(2)	0.06	6.95
0.5	387.92(4)	0.46	6.66
0.5 hp	386.86(5)	0.11	6.92
1.0	388.87(2)	0.54	6.73
1.0 hp	388.44(1)	0.33	6.84
1.5	389.63(4)	0.60	6.85
1.5 hp	389.43(2)	0.41	6.90

Mössbauer spectroscopy

Variable-temperature Mössbauer investigations have been performed on high-pressure oxygen annealed samples of $Sr_3Fe_{2-x}Ti_xO_{7-y}$ with $x=0.2$, 0.5 and 1.0. In view of the low magnetic ordering temperature (see below) and the small Fe content the material with $x=1.5$ was characterized only by room-temperature Mössbauer spectroscopy. Mössbauer spectra of the sample with $x=0.2$ are depicted in Fig. 2. The spectra at 4 and 20 K reveal a magnetic hyperfine splitting and can be described by two sextets with an intensity ratio of approximately 1 : 1. The parameters obtained from the evaluation of the low-temperature spectra (isomer shifts δ, magnetic hyperfine fields B_{hf}, and quadrupole interaction parameters ε)

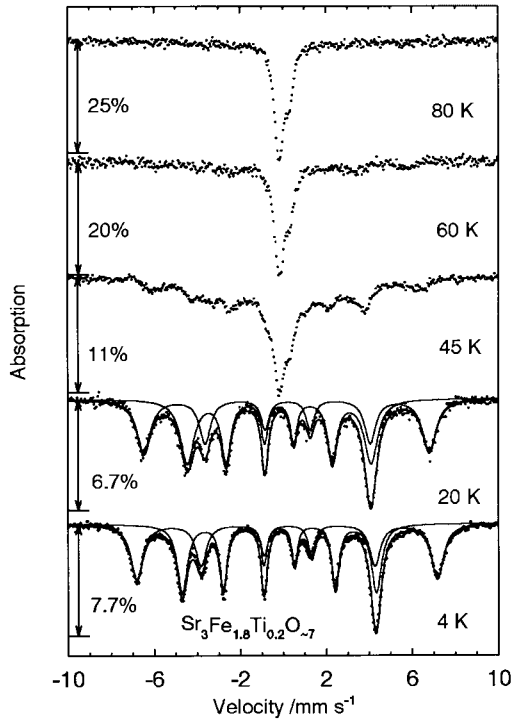

Fig. 2 Mössbauer spectra of $Sr_3Fe_{1.8}Ti_{0.2}O_{\sim 7}$ in the magnetically ordered phase and in the temperature range of the phase transition.

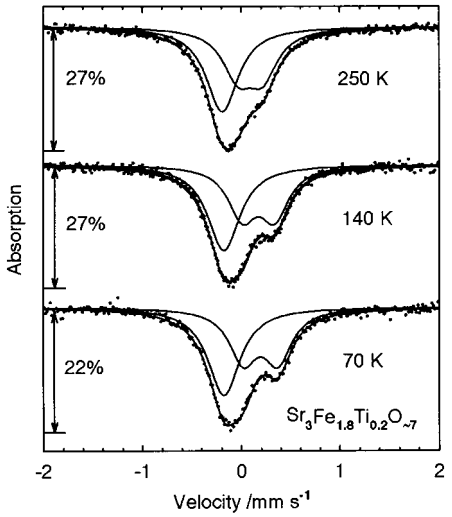

Fig. 3 Mössbauer spectra of $Sr_3Fe_{1.8}Ti_{0.2}O_{\sim 7}$ in the paramagnetic phase.

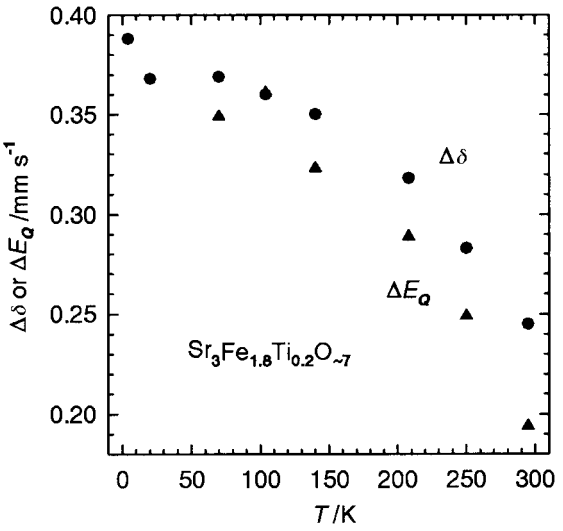

Fig. 4 Temperature dependence of the quadrupole splitting ΔE_Q of site I and the difference $\Delta\delta$ in isomer shifts between the two sites in the Mössbauer spectra of $Sr_3Fe_{1.8}Ti_{0.2}O_{\sim 7}$.

are summarized in Table 2. The 45 K spectrum evidences the coexistence of magnetically ordered and paramagnetic sites, but the lines of the former are strongly broadened. In the 60 and 80 K spectra the magnetic hyperfine structure is not resolved. However, it is seen from the absorption scale in Fig. 2 that a broad magnetic background is still present. Representative spectra in the paramagnetic phase which were measured with a smaller velocity range are shown in Fig. 3. The spectra become more structured with decreasing temperature. As there is no unambiguous analysis of these spectra the presence of two sites with a relative abundance of 1 : 1 as in the low-temperature spectra was assumed. Site I shows a small positive isomer shift and a quadrupole splitting, whereas site II has a small negative isomer shift and apparently gives rise to a single line (see Table 2). The temperature dependence of the quadrupole splitting ΔE_Q of site I and of the difference $\Delta\delta$ in the isomer shifts between the two sites are depicted in Fig. 4.

Mössbauer spectra of the phases with higher Ti concentrations are shown in Fig. 5 ($x=0.5$) and 6 ($x=1.0$), respectively. Again, the low-temperature spectra were analyzed as two hyperfine sextets. It is obvious from the parameters in Table 2 that the differences $\Delta\delta$ in isomer shifts and ΔB in hyperfine fields between the two sites are considerably larger for Sr_3FeTiO_{7-y} than for the other two materials. The area fraction of site I decreases with increasing Ti content x. Also the temperature T_m where a magnetic hyperfine pattern

Table 2 Mössbauer parameters of $Sr_3Fe_{2-x}Ti_xO_{7-y}$. The units are mm s^{-1} for the isomer shifts δ, the quadrupole splittings ΔE_Q, and the quadrupole splitting parameters ε of the magnetically ordered phase, and Tesla for the magnetic hyperfine fields B_{hf}. The statistical errors from the fits are <1 in the last digit if not explicitely given in parentheses

		$x=0.2$, $y=0.05$		$x=0.5$, $y=0.08$		$x=1.0$, $y=0.16$		$x=1.5$, $y=0.10$
		293 K	4 K	293 K	5 K	293 K	2 K	293 K
Site I	δ	0.17	0.33	0.21	0.33	0.27	0.39(2)	0.36(4)
	ε rsp. ΔE_Q	0.19	−0.02	0.21(2)	0.01	0.24(2)	−0.01(1)	0.24(5)
	B_{hf}		43.3		43.6		46.7(2)	
	Area (%)	50[a]	49(1)	45[a]	45(2)	41[a]	41(2)	32(5)
Site II	δ	−0.08	−0.05	−0.09	−0.06	−0.11	−0.07(1)	−0.09(2)
	ε rsp. ΔE_Q			0.15(2)		0.19		0.21(2)
	B_{hf}		28.0		27.7		27.1(1)	
	Area (%)	50[a]	51(1)	55[a]	55(2)	59[a]	59(2)	68(5)
	$\Delta\delta$	0.25	0.38	0.30	0.39	0.38	0.46	0.45
	ΔB		15.3		15.9		19.6	

[a]Parameter was not varied.

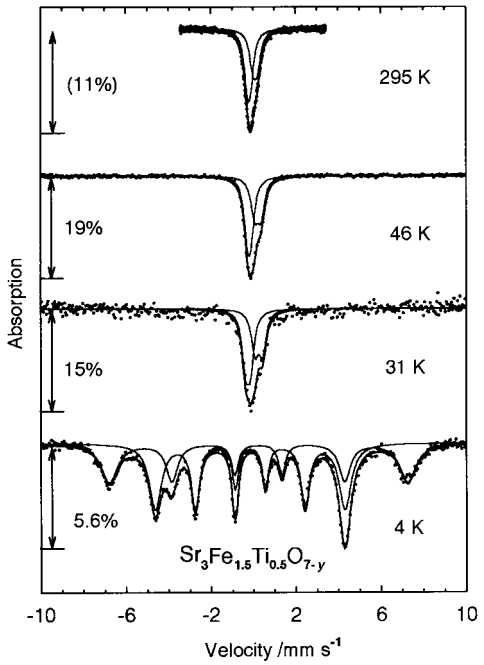

Fig. 5 Mössbauer spectra of $Sr_3Fe_{1.5}Ti_{0.5}O_{7-y}$ at various temperatures. Note that the room-temperature spectrum was measured with a different equipment.

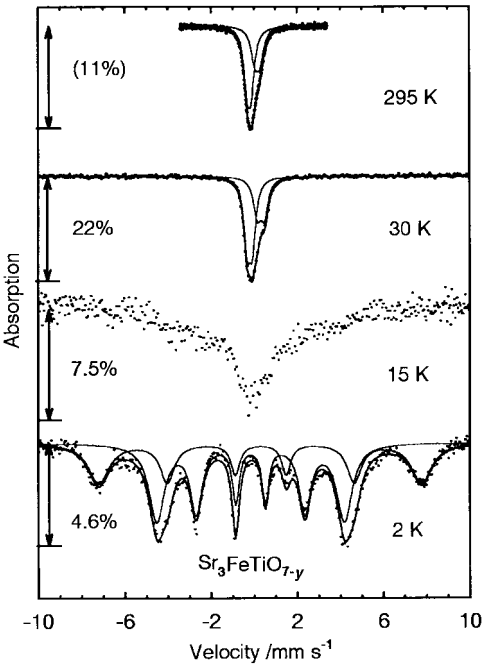

Fig. 6 Mössbauer spectra of Sr_3FeTiO_{7-y} at various temperatures. Note that the room-temperature spectrum was measured with different equipment.

becomes apparent in the Mössbauer spectra decreases with increasing x. The spectra of the paramagnetic phases have been analyzed by assuming quadrupole doublets for sites I and II, respectively, their area fractions being restricted to the values obtained from the low-temperature spectra. Comparison of the isomer shift data at room temperature (Table 2) shows that as in the low-temperature spectra the difference in the isomer shifts between the two sites increases with increasing x. The room-temperature Mössbauer spectrum of $Sr_3Fe_{0.5}Ti_{1.5}O_{7-y}$ (not shown) was analyzed by two quadrupole doublets with variable intensities.

Table 3 Results from magnetic susceptibility measurements on $Sr_3Fe_{2-x}Ti_xO_{7-y}$. T_m corresponds to the temperature of the maximum in the zfc–$\chi(T)$ curves. Magnetic moments μ_{eff} and Θ parameters were derived from a Curie–Weiss plot between 240 and 300 K

x	μ_{eff}/μ_B	Θ/K	T_m/K
0.2	6.6	63	65
0.5	6.3	77	20
1.0	6.0	71	11
1.5	5.6	64	3

Magnetic susceptibility measurements

In Fig. 7 the molar magnetic susceptibilities χ and their inverses χ^{-1} of the $Sr_3Fe_{2-x}Ti_xO_{7-y}$ samples are depicted as a function of temperature. A broad maximum in the $\chi(T)$ curve of $Sr_3Fe_{1.8}Ti_{0.2}O_{7-y}$ centered around 65 K indicates antiferromagnetic behavior with a gradual transition to the magnetically ordered state. Below 30 K ZFC and FC data are different. A gradual transition to the magnetically ordered phase compares well with the Mössbauer spectra depicted in Fig. 2. In the $\chi(T)$ data of $Sr_3Fe_{1.5}Ti_{0.5}O_{7-y}$ a maximum is seen only in the ZFC curve below 20 K but not in the FC curve. Above 20 K FC and ZFC data are in good agreement. Similarly, a divergence of FC and ZFC $\chi(T)$ curves below 10 and 4 K is observed for Sr_3FeTiO_{7-y} and $Sr_3Fe_{0.5}Ti_{1.5}O_{7-y}$, respectively. In all cases $\chi^{-1}(T)$ deviates from a straight line and thus does not follow a Curie–Weiss law $\chi(T)=C/(T-\Theta)$ over extended temperature ranges. Using the $\chi^{-1}(T)$ data between 240 and 300 K one obtains magnetic moments μ_{eff} which are larger than the spin-only value for a d^4 high-spin configuration (4.9 μ_B) of a single ion and positive Θ parameters for all the materials (see Table 3). The values for μ_{eff} decrease with increasing x.

Electrical resistance measurements

In Fig. 8 the logarithm of the electrical conductivity σ is depicted as a function of inverse temperature for $Sr_3Fe_{2-x}Ti_xO_{7-y}$ samples with $x=0.2$, 0.5 and 1.0 together with the data for $Sr_3Fe_2O_7$ from ref. 3. The data for $x=0.2$ reveal, similar to the case of the unsubstituted material, that the conductivity at low temperatures is only weakly activated whereas the activation energy becomes larger at higher temperatures. The low-temperature conductivity decreases by several orders of magnitude with increasing x.

4 Discussion

The powder X-ray diagrams of the present $Sr_3Fe_{2-x}Ti_xO_{7-y}$ samples reveal that the tetragonal Ruddlesden–Popper-type crystal structure of the parent compounds $Sr_3Fe_2O_{7-y}$ and $Sr_3Ti_2O_7$ is retained for all values of x and y. From the non-linear increase in the lattice constant a with x it is concluded that in spite of annealing the materials at high oxygen pressures a certain oxygen deficiency giving rise to partial reduction of Fe^{IV} to Fe^{III} could not be avoided. The Fe^{III} fractions were estimated from the a-lattice parameters according to eqn. (1) where the validity of Vegard's law has been assumed. Indeed, a linear increase of a with increasing y or equivalently with increasing Fe^{III} fraction was found for the system $Sr_3Fe_2O_{7-y}$ by neutron diffraction studies.[12] From the data in Table 1 it is seen that the Fe^{III} fraction increases with increasing x which is also in agreement with the smaller change in a per Fe atom after high-pressure oxygen annealing for the materials with larger x. This is attributed to the fact that the ionic radius of Ti^{IV} is larger than that of Fe^{IV}. Accordingly, the incorporation of larger Fe^{III} ions into the crystal structure is favored with increasing x. A discussion of the properties of the present materials must therefore include the effects arising from

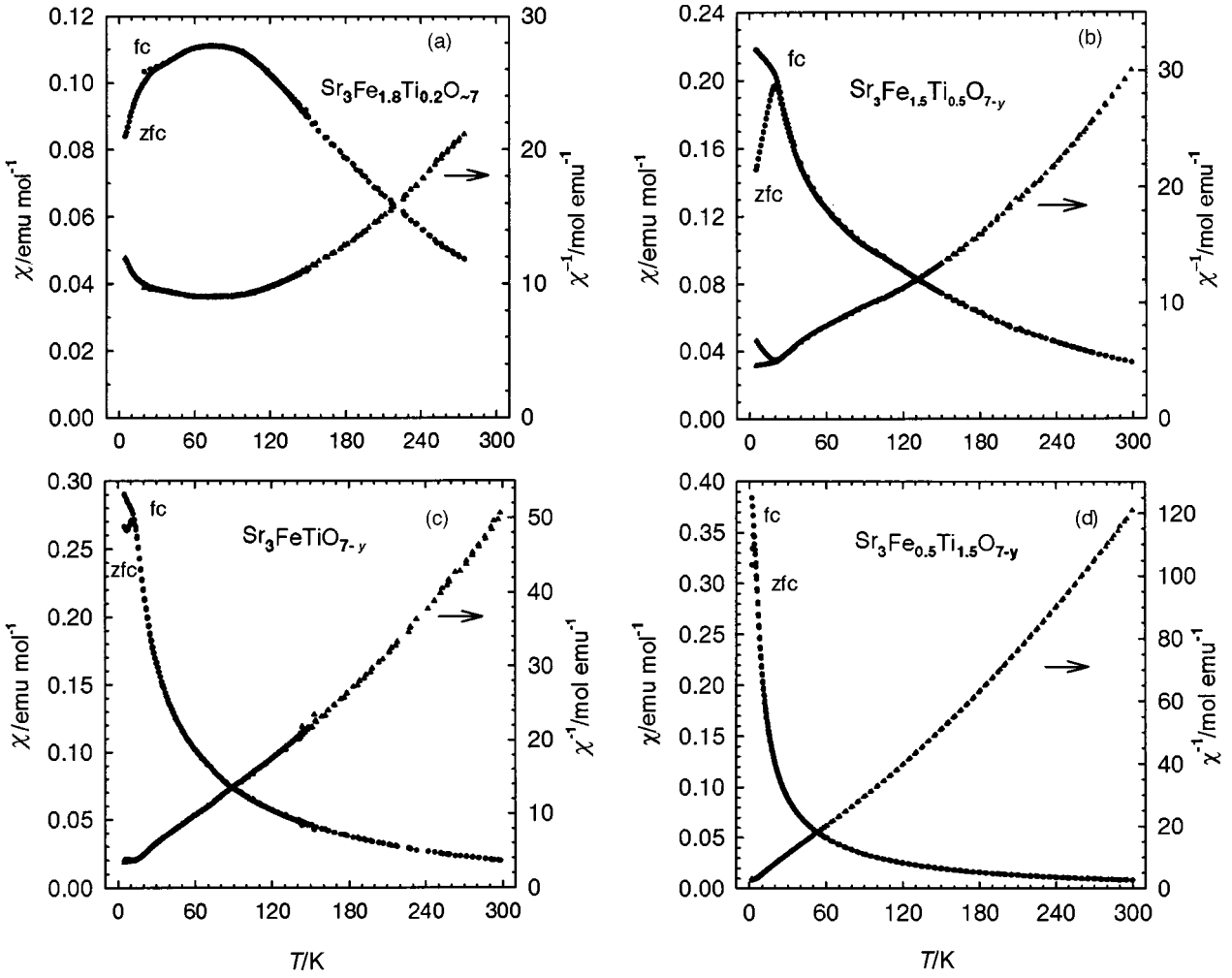

Fig. 7 Molar magnetic susceptibilities χ of $Sr_3Fe_{2-x}Ti_xO_{7-y}$ and their inverses χ^{-1} as a function of temperature: (a) $x=0.2$, (b) $x=0.5$, (c) $x=1.0$, (d) $x=1.5$.

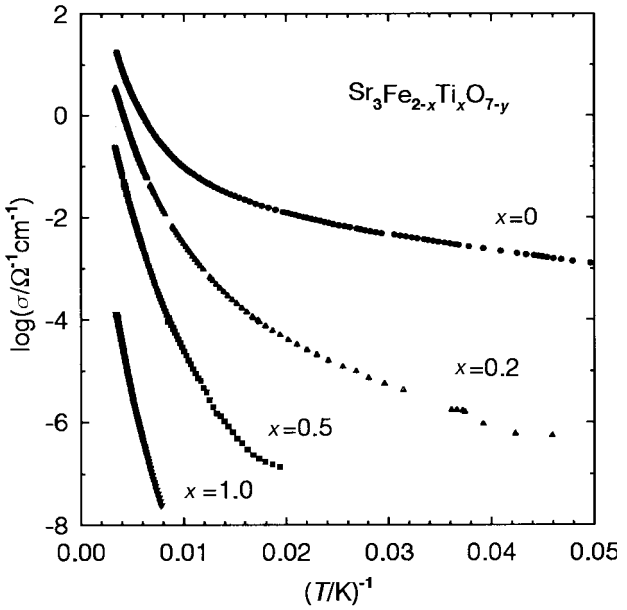

Fig. 8 Electrical conductivities of $Sr_3Fe_{2-x}Ti_xO_{7-y}$ as a function of inverse temperature. The data for $x=0$ were taken from ref. 3.

Fe^{III}/Fe^{IV} mixed valency and the variation in coordination numbers of the transition metal ions in addition to the effects caused by dilution of the Fe–O network with Ti. In oxygen-deficient $Sr_3Fe_2O_{7-y}$ the O(3) atoms combining two perovskite slabs in the crystal structure are removed.[12] Each oxygen vacancy leads to two five-coordinate Fe ions.

In $Sr_3Fe_{1.8}Ti_{0.2}O_{7-y}$ oxygen deficiency is still small and the inherent Fe^{III} contribution of about 6% is not larger than for the samples of $Sr_3Fe_2O_{\sim 7}$ and $Sr_{2.7}Ba_{0.3}Fe_2O_{\sim 7}$ which have been investigated in our previous study.[3] Similar to $Sr_3Fe_2O_{\sim 7}$ the low-temperature Mössbauer spectra of $Sr_3Fe_{1.8}Ti_{0.2}O_{\sim 7}$ are composed of two hyperfine sextets with an intensity ratio of approximately 1 : 1. It is concluded that the charge disproportionation of Fe^{IV} persists in this material. If the charge disproportionation is formulated with integral oxidation states site I (positive isomer shift) is assigned to Fe^{III} and site II (negative isomer shift) to Fe^{V} ions. However, the differences $\Delta\delta$ in isomer shifts and ΔB in hyperfine fields between the two sites are only about half of the corresponding differences for octahedrally coordinated Fe^{III} and Fe^{V} oxides.[3] This result suggests a rather gradual charge-density and spin-density modulation even in materials where all Fe ions are formally in the +4 oxidation state. Most remarkably, for $Sr_3Fe_{1.8}Ti_{0.2}O_{\sim 7}$ $\Delta\delta$ is about 0.05 mm s^{-1} and ΔB about 2 T larger than for the unsubstituted material ($\Delta\delta=0.33$ mm s^{-1}, $\Delta B=13.4$ T). As the Fe^{III} fractions are not very different it is concluded that the disturbance of the Fe-O network accompanying the substitution of Fe^{IV} by Ti^{IV} ions leads to a

stronger degree of charge and spin separation between the two Fe sites. In this respect $Sr_3Fe_{1.8}Ti_{0.2}O_{\sim 7}$ behaves differently from $Sr_{2.7}Ba_{0.3}Fe_2O_{\sim 7}$ where 10% of the electronically inactive Sr^{2+} sites were replaced by Ba^{2+}.[3] In the latter material both, $\Delta\delta$ and ΔB were nearly the same as for $Sr_3Fe_2O_{\sim 7}$. The charge disproportionation of Fe^{IV} is also evident in the Mössbauer spectra of the paramagnetic phase of $Sr_3Fe_{1.8}Ti_{0.2}O_{\sim 7}$. The analysis of the spectra reveals a similar temperature dependence of $\Delta\delta$ and of ΔE_Q for site I (Fig. 4) as for $Sr_3Fe_2O_{\sim 7}$.[3] The temperature dependence of $\Delta\delta$ is more pronounced than expected for differences in the second-order Doppler shift between the two sites. As has been discussed in ref. 3 the temperature dependence of $\Delta\delta$ and ΔE_Q may indicate that the degree of charge separation in the paramagnetic phase is somewhat temperature dependent. A complete disappearance of the charge disproportionation above 290 K was observed for the classical system $CaFeO_3$.[10]

A slightly increased Fe^{III} fraction of about 11% due to oxygen deficiency was derived from the *a*-lattice parameter of $Sr_3Fe_{1.5}Ti_{0.5}O_{7-y}$, which again is much smaller than the area fraction of site I in the low-temperature Mössbauer spectrum. These results suggest that there is still a charge disproportionation of Fe^{IV} which is also in agreement with the Mössbauer parameters. The values for $\Delta\delta$ and ΔB are only slightly larger than for $Sr_3Fe_{1.8}Ti_{0.2}O_{\sim 7}$. However, the area fraction of site I of about 45% is considerably smaller than the fraction of 55% Fe^{III} like sites which is expected if all Fe^{IV} sites are assumed to participate in the charge disproportionation. It is noted in this context that also for $Sr_3Fe_2O_7$ the area ratio of 1 : 1 is only observed well below the magnetic ordering temperature whereas in the temperature range of the magnetic phase transition the fraction of Fe^{III} like sites decreases.[3] Spin fluctuations could be the reason for this observation. In the Ti-substituted materials the onset of magnetic ordering effects in the Mössbauer spectra occurs at lower temperatures as the exchange pathways are disturbed. The room-temperature Mössbauer spectrum of $Sr_3Fe_{1.5}Ti_{0.5}O_{7-y}$ can be described by restricting the intensity ratio between the two sites to the low-temperature value, but it is also well compatible with a fraction of 55% Fe^{III} and 45% Fe^{V} like sites. On the other hand, the shape of the spectrum cannot be reproduced by assuming a mixed valency with 89% Fe^{IV} and 11% Fe^{III}.

The low-temperature Mössbauer spectrum of Sr_3FeTiO_{7-y} is again reasonably described by two broadened hyperfine sextets. In contrast to the samples with $x=0.2$ and 0.5 the area fraction of site I is comparable to the Fe^{III} fraction estimated from the X-ray powder data. Both, the differences in $\Delta\delta$ and ΔB have increased considerably (Table 2) and are similar to those in the perovskite system $SrFe_{1-x}Ti_xO_{3-y}$, namely in $Sr_2FeTiO_{5.81}$[14] and $SrFe_{0.7}Ti_{0.3}O_{3-y}$[15] where a charge disproportionation of Fe^{IV} can be ruled out. The room-temperature spectrum of Sr_3FeTiO_{7-y} can be well reproduced by 40% Fe^{III} and 60% Fe^{IV} sites as in the low-temperature spectrum. Its shape is, however, incompatible with the presence of 67% Fe^{III} and 33% Fe^{V} like sites expected for a charge disproportionation of Fe^{IV}. It is concluded that the Mössbauer spectra of Sr_3FeTiO_{7-y} rather reflect a conventional Fe^{III}/Fe^{IV} mixed valency as formally derived from sample composition than a charge disproportionation of Fe^{IV}. In particular, the values of δ and B_{hf} for site I are compatible with an assignment to five-coordinate Fe^{III} sites which are formed in the vicinity of oxygen vacancies. The corresponding parameters for sites I in the Mössbauer spectra of the charge disproportionation phases are smaller. The broadening of the sextets in the low-temperature spectrum suggests a distribution of hyperfine fields as the degree of broadening increases from the inner towards the outer lines. This is not unusual for disordered solid solutions and is attributed to the variations in the local environments of the Fe centers. Also the Fe^{III} area fraction obtained from the room-temperature Mössbauer spectrum of $Sr_3Fe_{0.5}Ti_{1.5}O_{7-y}$ is in reasonable agreement with the Fe^{III} fraction derived from the X-ray data.

For discussing the results from Mössbauer spectroscopy on $Sr_3Fe_{2-x}Ti_xO_{7-y}$ it is useful to sketch the electronic situation in perovskite-related Fe^{IV} oxides. The electronic behavior of transition metal oxides may be rationalized in terms of two main energies: the intra-atomic electron–electron correlation energy U within the partially filled d shell (Coulomb repulsion and exchange energy) which favors localization of the d electrons and the electron-transfer energy resulting from covalent M 3d–O 2p–M 3d interactions which gives rise to a conduction band of width w.[16] In iron(IV) oxides there are strong correlation effects due to the large number of unpaired d electrons but there is also a pronounced tendency for electron transfer due to strong covalency of chemical bonding for this high oxidation state of iron. The competition between these two effects leads to the manifold of electronic behavior encountered in this class of compounds. In an octahedral ligand field of oxygen ions the five Fe 3d orbitals are split into a set of three t_{2g} orbitals which are Fe 3d–O 2p π^* antibonding and two e_g orbitals which are Fe 3d–O 2p σ^* antibonding. As the π interactions are weaker than the σ interactions it may be assumed that the π^* electrons are still localized whereas the σ^* orbitals form a narrow conduction band of width w_σ. It has been argued that perovskite-related Fe^{IV} oxides are transition metal oxides at the insulator–metal borderline.[2,3] A collective charge-disproportionation state may be formed in a certain range of ratios w_σ/U prior to the insulator–metal transition. In addition, electron–phonon interaction is likely to be important for the stabilization of the charge disproportionation of Fe^{IV}. In fact, neutron diffraction[17] and recent electron diffraction[18] experiments on $La_{0.3}Sr_{0.7}FeO_3$ (formally 67% Fe^{IV} and 33% Fe^{III}), a material with a charge disproportionation in the magnetically ordered phase, suggest spin and charge ordering with an accompanying structural modulation in this compound. Substitution of Fe^{IV} by Ti^{IV} in $Sr_3Fe_2O_7$ reduces the number of M 3d–O 2p–M 3d electron-transfer pathways and thus the band width w_σ. One could expect a breakdown of the charge disproportionation for Ti concentrations larger than a critical value x_c. A direct test of this conjecture is, however, not possible as the properties of the present materials are complicated by the occurrence of oxygen vacancies which formally leads to Fe^{III}/Fe^{IV} mixed-valence compounds. In contrast to oxomanganates the itineracy of the electronic system in Fe^{III}/Fe^{IV} mixed-valence materials is reduced in comparison with the parent compound.[3,4,11] In addition, the impurity potentials arising from the various kinds of defects tend to localize the σ^* electrons. These effects together lead to a decrease of the electrical conductivity with increasing Ti content (Fig. 8). In $Sr_3Fe_{1.8}Ti_{0.2}O_{\sim 7}$ and $Sr_3Fe_{1.5}Ti_{0.5}O_{7-y}$ the electron-transfer pathways appear still to be intact enough to maintain a collective charge-disproportionation state. The Mössbauer parameters suggest that the differences in charge and spin density between the two Fe sites are larger than in $Sr_3Fe_2O_7$ where the Fe–O network is undisturbed. In $Sr_3Fe_{2-x}Ti_xO_{7-y}$ with $x=1$, 1.5 the larger Ti and Fe^{III} concentrations reduce the electron-transfer tendency further which leads to the formation of a Fe^{III}/Fe^{IV} mixed-valence state rather than to a charge disproportionation of Fe^{IV}.

The magnetism of the system $Sr_3Fe_{2-x}Ti_xO_{7-y}$ is characterized by deviations from simple Curie–Weiss behavior, positive Θ temperatures, magnetic moments which are larger than the spin-only value expected for a d^4 high-spin ion, and antiferromagnetic ordering for $x=0.2$ or a divergence of FC and ZFC susceptibility curves at low temperatures for larger x. These results suggest that as in unsubstituted strontium ferrates(IV) the magnetism is governed by a competition between ferro- and antiferro-magnetic exchange interactions.

Since the σ* electrons are reasonably discussed in terms of collective-electron behavior the ferromagnetic interactions are attributed to the tendency to delocalize the σ* electrons in the narrow conduction band.[3] Adopting the picture of a charge disproportionation in $Sr_3Fe_{2-x}Ti_xO_{7-y}$ for $x \leqslant 0.5$ the relevant charge-fluctuation process in these materials may be formulated as

$$(\pi^*)^{\uparrow\uparrow\uparrow}(\sigma^*)^0 + (\pi^*)^{\uparrow\uparrow\uparrow}(\sigma^*)^{\uparrow\uparrow} \rightarrow 2(\pi^*)^{\uparrow\uparrow\uparrow}(\sigma^*)^{\uparrow} \qquad (2)$$

which is favored when the magnetic moments at adjacent Fe sites are ferromagnetically aligned. This corresponds to the double-exchange mechanism for ferromagnetic interactions in mixed-valence metal oxides.[19] On the other hand, antiferromagnetic interactions occur between the half-filled more localized $(\pi^*)^3$ subshells. The small activation energy for electron conduction at low temperatures in $Sr_3Fe_2O_7$ and some of the substituted materials (see Fig. 8 and ref. 3) may reflect the more probable electron transfer in the magnetically ordered phase. A similar behavior has been observed recently in the oxygen-deficient $SrFeO_{3-y}$ system.[20] Substitution of Fe^{IV} ions by Ti^{IV} and Fe^{III} ions disturbs the exchange pathways and the balance between ferro- and antiferromagnetic interactions. This leads to a lower average magnetic ordering temperature for $Sr_3Fe_{1.8}Ti_{0.2}O_{\sim 7}$. Actually a distribution of ordering temperatures occurs. This is suggested by the broad maximum in the magnetic susceptibility curve and by the coexistence of paramagnetic and magnetically ordered sites over a quite large temperature range as seen in the Mössbauer spectra. Also in the more diluted compounds investigated in this study the magnetism does not reflect single-ion behavior. Even at elevated temperatures magnetic clusters involving still ferromagnetic interactions are formed. With increasing x the fraction of Fe^{III} sites increases due to increasing oxygen deficiency. These sites give rise to additional antiferromagnetic exchange interactions. The disorder introduced by mixing Fe^{IV}, Fe^{III} and Ti^{IV} ions and the competition between ferro- and antiferromagnetic interactions lead to frustration effects which prevent the development of long-range magnetic order and give rise to spin-glass behavior. This is probably the origin of the divergence of FC and ZFC magnetic susceptibility curves at low temperatures. Spin-glass behavior has been found previously in the related perovskite system $Sr_2FeTiO_{5.81}$.[14] In the latter material which was not annealed at high oxygen pressure antiferromagnetic interactions seem to be more pronounced as is suggested by the smaller magnetic moment ($\mu_{eff} = 4.6\ \mu_B$) and by the slightly negative Θ value ($\Theta = -20$ K).

5 Conclusions

Our studies on the system $Sr_3Fe_{2-x}Ti_xO_{7-y}$ support an interpretation of the charge disproportionation of Fe^{IV} in these and related materials as a collective electronic state with partial transfer of charge and spin density between the different Fe sites in the solid. This is suggested by the detailed inspection of the Mössbauer isomer shifts and hyperfine fields which are sensitive probes for the charge and spin density at the transition metal site. It is particularly noteworthy that the differences in isomer shifts and hyperfine fields and accordingly in charge and spin densities between the two sites in the charge-disproportionation phase of $Sr_3Fe_2O_7$ are smaller than for the Fe^{III} and Fe^{IV} sites in Sr_3FeTiO_{7-y}. The charge disproportionation in Fe^{IV} oxides is often described in terms of Fe^{III} and Fe^{V} sites which qualitatively would suggest larger differences in charge and spin density. Substitution of Fe^{IV} by Ti^{IV} and the accompanying reduction of some Fe^{IV} to Fe^{III} due to oxygen deficiency decrease the tendency for electron transfer in the system $Sr_3Fe_{2-x}Ti_xO_{7-y}$ which for materials with $x \geqslant 1$ leads to the disappearance of the charge disproportionation. Further studies on Fe^{IV} oxides are promising with respect to illuminating the interplay between crystal structure, electronic state, magnetism, electronic conduction, and electron–lattice interactions in transition metal oxides, in particular as Fe^{IV} is isoelectronic with Mn^{III} which occurs in many of the CMR materials.

Acknowledgments

I am grateful to E. Brücher and N. Rollbühler for performing the magnetic susceptibility and electrical resistance measurements, and to W. Hölle for assistance with sample preparation and characterization. I thank Professor P. Gütlich, University of Mainz, for the possibility to measure low-temperature Mössbauer spectra in his laboratory and to Dr. J. Ensling for his support during the experiments. Furthermore, I gratefully acknowledge a fellowship of the Deutsche Forschungsgemeinschaft during part of this work.

References

1 D. I. Khomskii and G. A. Sawatzky, *Solid State Commun.*, 1997, **102**, 87.
2 P. Adler, A. F. Goncharov and K. Syassen, *Hyperfine Interact.*, 1995, **95**, 71.
3 P. Adler, *J. Solid State Chem.*, 1997, **130**, 129.
4 J. B. MacChesney, R. C. Sherwood and J. F. Potter, *J. Chem. Phys.*, 1965, **43**, 1907.
5 T. Takeda, Y. Yamaguchi and H. Watanabe, *J. Phys. Soc. Jpn.*, 1972, **33**, 967.
6 S. E. Dann, M. T. Weller, D. B. Currie, M. F. Thomas and A. D. Al-Rawwas, *J. Mater. Chem.*, 1993, **3**, 1231.
7 P. Adler, *J. Solid State Chem.*, 1994, **108**, 275.
8 P. Adler, A. F. Goncharov, K. Syassen and E. Schönherr, *Phys. Rev. B*, 1994, **50**, 11396.
9 G. R. Hearne, M. P. Pasternak and R. D. Taylor, *Nuovo Cimento*, 1996, **18**, 145.
10 M. Takano, N. Nakanishi, Y. Takeda, S. Naka and T. Takada, *Mater. Res. Bull.*, 1977, **12**, 923.
11 M. Takano and Y. Takeda, *Bull. Inst. Chem. Res. Kyoto Univ.*, 1983, **61**, 406.
12 S. E. Dann, M. T. Weller and D. B. Currie, *J. Solid State Chem.*, 1992, **97**, 179.
13 M. M. Elcombe, E. H. Kisi, K. D. Hawkins, T. J. White, P. Goodman and S. Metheson, *Acta Crystallogr., Sect. B*, 1991, **47**, 305.
14 T. C. Gibb, P. D. Battle, S. K. Bollen and R. J. Whitehead, *J. Mater. Chem.*, 1992, **2**, 111.
15 P. Adler, *Investigations on the Nature of Electronic States and Properties of Oxocuprates and Oxoferrates*, Habilitationsschrift, Stuttgart, Mainz, 1996, available on request.
16 J. B. Goodenough, *Prog. Solid State Chem.*, 1971, **5**, 145.
17 P. D. Battle, T. C. Gibb and P. Lightfoot, *J. Solid State Chem.*, 1990, **84**, 271.
18 J. Q. Li, Y. Matsui, S. K. Park and Y. Tokura, *Phys. Rev. Lett.*, 1997, **79**, 297.
19 C. Zener, *Phys. Rev.*, 1951, **82**, 403.
20 S. Nakamura and S. Ida, *Jpn. J. Appl. Phys.*, 1995, **34**, L 291.

Paper 8/06772D